

Internal Granular Dynamics, Shear-Induced Crystallization, and Compaction Steps

J.-C. Tsai,¹ G. A. Voth,² and J. P. Gollub^{1,2}

¹*Physics Department, University of Pennsylvania, Philadelphia, Pennsylvania 19104, USA*

²*Physics Department, Haverford College, Haverford, Pennsylvania 19041, USA*

(Received 11 March 2003; published 6 August 2003)

Internal imaging using index matching, and sensitive volume measurement, are used to investigate the spatial order and dynamics of a deep disordered layer of spheres sheared under a fixed load. Shearing triggers a crystallization transition accompanied by a step compaction event. The delay preceding the transition depends strongly on the layer thickness and can require a translation of about 10^5 particle diameters. The mean velocity varies with depth by more than five decades, and its profile is qualitatively altered by the transition.

DOI: 10.1103/PhysRevLett.91.064301

PACS numbers: 45.70.Cc, 83.50.Ax, 83.80.Hj, 64.60.Cn

The response of granular material to imposed shear is a key to understanding granular dynamics. Since internal spatial structure can affect flow rheology, it is important to monitor the internal grain motion and rearrangement. Work on colloidal suspensions has shown that imposed shear can lead to internal ordering. The implications of this phenomenon for granular dynamics, where the particles are much larger and not subject to thermal excitation, remain unclear, in part because internal structure is difficult to determine.

There have been previous studies of sheared dense granular flows. Mueth *et al.* [1] used MRI and x-ray tomography to study the internal velocity of a Couette flow with a thickness about six grain diameters. Profiles of mean density and mass flow rate were obtained with subgrain resolution to understand the generic structure of the “shear band,” a narrow region of a few grain diameters that is substantially mobilized by boundary driving. For gravity-driven dense flows, Komatsu *et al.* provided indirect evidence from video imaging of grains near a flat confining surface [2] suggesting that the mobile region can penetrate deeply into the granular material. Numerical simulations allow probing of the 3D structure and time evolution inside densely packed steady flows [3,4], but the difficulty of obtaining experimental information about interior grain rearrangement currently limits theoretical progress on dense granular flows [5–7].

A number of computer simulations have demonstrated crystalline ordering of hard spheres under steady shearing [8–11]. In simulations at constant granular temperature, an ordering transition occurs when the shear rate exceeds a critical value set by the mean collision time [8,9]. Simulations that include the interaction between grains and interstitial fluid [11] show ordering that depends on the filled volume fraction and can be delayed by increasing the intergrain friction. Soft sphere simulations of gravity-driven granular flows [3] have observed oscillating crystallization on an ordered boundary. Experiments using light scattering and video microscopy [12,13] reveal the rheological response of ordered colloidal suspen-

sions to finite or oscillatory strain. Although ordering has been seen in granular systems [14], its role has remained unclear since the strongly nonlinear velocity profile and interparticle friction can delay ordering, and it is often suppressed by sufficient polydispersity. As a result, models of granular rheology typically ignore ordering [5–7].

In this work, we combine a novel internal imaging technique and sensitive measurement of granular volume to investigate the internal spatial structure and time evolution of a deep boundary-driven flow. Velocity profiles are measured with a dynamic range of 10^5 . We find that steady shearing under constant normal load in an annular plane Couette geometry triggers a crystallization transition that is accompanied by a step compaction event. While crystallization for a packing with small polydispersity may perhaps be anticipated, the experiments reveal a wealth of phenomena that have not been seen previously. The transition occurs after a delay that can be long and depends strongly on layer thickness. It leads to substantial change in the rheology of the material, as indicated by the structure of the internal velocity field, measured here in three dimensions.

Our system is a planar channel in an annular geometry (Fig. 1). Spherical glass beads of diameter $d = 0.6$ mm (with a standard deviation of 4%) fill the annular channel between two smooth concentric glass cylinders that are stationary, with filling height adjustable from a few grain diameters to $50d$. The channel width is about $30d$ and has a circumference of about $800d$. Glass beads are driven by the ring-shaped upper boundary, which is assembled on a precision bearing that allows free vertical movement while maintaining constant speed of rotation. Both the moving upper boundary and the static lower boundary are roughened by gluing a layer of the same glass beads at about the maximal area density; this produces the shearing schematically shown in the inset of Fig. 1. The weight W of the upper boundary assembly provides a constant normal load, which is more than 10 times the total weight of the grains at a typical filling height ($\approx 24d$), taking into account buoyancy effects.

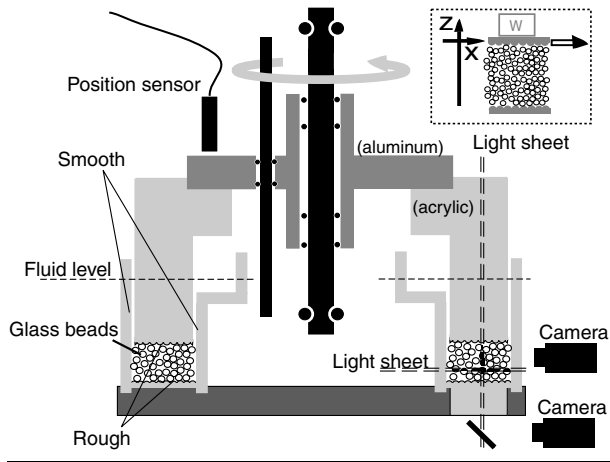


FIG. 1. Cross section of the annular plane shear flow, with an inset showing coordinates. The shear and normal load are provided by a rotating aluminum-acrylic assembly that is free to move vertically while maintaining a constant rotation rate. Both vertical and horizontal slices are imaged.

To image the interior, the interparticle space is filled with a special hydrocarbon mixture (viscosity ≈ 10 cS, density ≈ 1 g/cc, from Cargille Laboratories), with refractive index fine-tuned to match that of the beads. A small amount of fluorescent dye (Exiton-P580) is blended in the fluid. A laser sheet, narrower than $d/2$, is introduced either vertically or horizontally to illuminate the interparticle space. Images of the resulting slices are captured by a video camera, either through the outer cylindrical wall or the bottom window. We use convolution methods to obtain sharp peaks of intensity corresponding to grain centers, and then compare the centers of peaks in consecutive frames to construct the 2D projection of grain trajectories to a precision of about 0.025 – $0.1 d$, depending on image magnification. An advantage of this annular plane Couette geometry (compared to a circular Couette cell with a rotating cylinder) is the elimination of free surfaces. By making the gaps between the driving ring and the cylindrical walls slightly narrower than $d/2$, all grains are confined while air or fluid can freely leak through the gaps as the height of the upper boundary changes. Therefore, the vertical motion of the upper boundary assembly, detected by an inductive position sensor, serves as a direct indicator of the volume change of the granular packing.

The measured mean velocity profile along a vertical plane inside the flow (Fig. 2) illustrates the wide range of local time scales at different depths. The vertical image plane is about $12d$ away from the outer cylindrical wall. The full profile is obtained by patching together multiple local measurements using a wide range of frame rates; each data point is based on a local average of more than 50 individual grains. With the flow driven at a speed $12 d/s$ from above, the local grain displacement time $T_d = (\langle V_x \rangle / d)^{-1}$ continuously varies from 0.1 s to a few

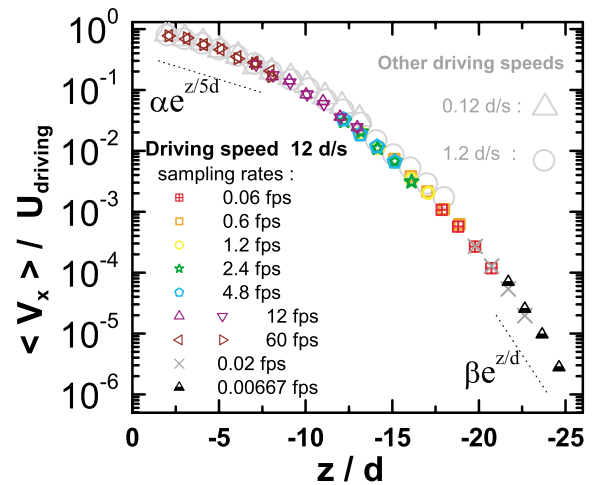


FIG. 2 (color online). Vertical profile of the time-averaged internal grain velocity in the final state (ordered layers). Velocities are normalized by the driving speed and plotted against height in units of the nominal particle diameter $d = 0.6$ mm, with $z = 0$ referring to the approximate position of the driving boundary. For the $12 d/s$ experiment, sampling rates (fps) are used to label data sets, in chronological order of measurement. The close match between the earliest and last set indicates that there is no drift over time. The scaled profile is rate independent.

hours from top to bottom, spanning more than five decades. This profile is based on the final state after a long time, in which the grains have aligned as 24 ordered layers throughout the cell [see Figs. 3(a) and 4(b)]; each data point in Fig. 1 represents the speed and mean height of a single horizontal layer. Although the grains pack nearly uniformly over the whole depth, the changing slope on this semilog plot indicates that the characteristic decay length gradually shrinks from roughly $5d$ at the top to $1d$ at the bottom. This changing slope may be a consequence of the grain weight, the effect of sidewalls, or the finite depth. The functional form of the final velocity profile is insensitive to a change of driving speed by a factor of 100, at least in the upper half of the flow. The time evolution of the velocity profile before the final state is reached will be discussed elsewhere.

The evolution of the flow structure from a disordered initial state during shear is striking. Constant-speed shearing under a fixed normal load consistently causes the grains to self-organize into ordered layers. For a thick-layer packing, this occurs generally after a delay with the accumulated boundary displacement as large as $10^5 d$. Figure 3 shows an ordering transition that creates the 24-layer state in Fig. 2. The compaction of the grains [shown in Fig. 3(b) after a short initial transient that depends on preparation] takes place at a highly nonuniform pace, and marks the ordering transition. The change of sample volume begins with a slow decrease, followed by a much steeper descent of about 2.5% as grains self-organize into ordered layers before reaching

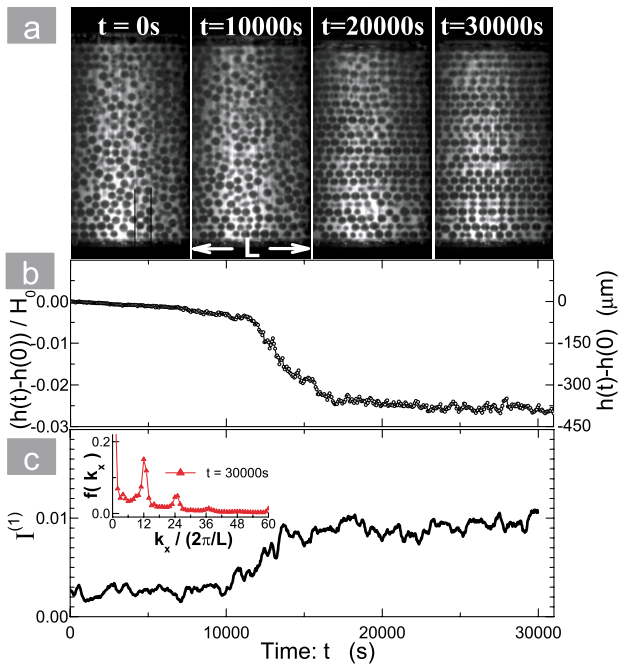


FIG. 3 (color online). Transition to the ordered state for a flow driven at 12 d/s . (a) Images of vertical internal slices at different times after the start of shearing. (b) Fractional volume compaction vs time, based on the change of height of the upper driving boundary. The actual change in microns is indicated at the right. (c) Simultaneous measure of internal order as indicated by the time-dependent intensity of the major peak of the spatial Fourier spectrum at longitudinal wave number $k_x/(2\pi/L) = 12$. The reference length L is marked in (a). The inset shows a sample spatial spectrum, as defined in the text, after ordering occurs.

a steady-state volume. The rate of descent during the transition varies stochastically in different runs and can be steeper; for example, compare the top two curves in Fig. 5. Note that the apparent grain size often alternates between the ordered rows in Fig. 3(a). This alternation indicates a displacement of adjacent layers consistent with hexagonal structure in planes perpendicular to the page. However, the filling fraction of the final state is about $(63 \pm 3)\%$, somewhat less than one might have anticipated for a hexagonal close packing.

To quantify the ordering, we first calculate the time-dependent normalized Fourier spectrum $f(k_x, t) = \langle |F(k_x, z, t)| / \|F\| \rangle_z$, in which the magnitude of the Fourier transform along x is divided by its norm $\|F\|$ to correct for possible fluctuations in light intensity, and is then averaged over the depth z ; then the intensity of the primary peak, $I^{(1)}$, is defined as the mean of f^2 within the peak width, after subtracting the broad background. The result [Fig. 3(c)] shows a step in the periodic order with respect to time, corresponding to the compaction.

Horizontal sliced images can be used to resolve the 3D structure of the flow. Under identical driving conditions, dramatic differences are found before and after the order-

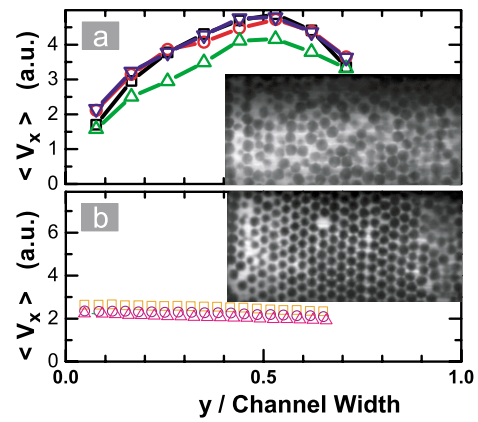


FIG. 4 (color online). Horizontal profiles of time-averaged internal grain velocity across the channel at midheight ($z = 12d$), in arbitrary units. (a) Disordered state and corresponding image; the grain velocity is Poiseuille-like with slip at the boundaries. (b) Ordered state and corresponding image. The grain velocity is nearly uniform across the image as the flow consists of nearly rigid sheets sliding over each other. Point defects and line dislocations are visible.

ing transition. In the disordered state [Fig. 4(a)], the grain velocity exhibits a significant decay towards the sidewalls. The ordered state [Fig. 4(b)] forms hexagonal sheets sliding against adjacent layers, and shows no significant decay of speed towards the sidewalls. Defects are visible, and point defects persist as they move across the field of view. Large regions move coherently, often in a zigzag pattern. A similar zigzag motion has been discussed in Ref. [12].

We also adjust the total quantity of glass beads contained in the cell, and find that the characteristic time to reach the final volume or to form ordered layers varies dramatically with mean thickness. Figure 5(a)

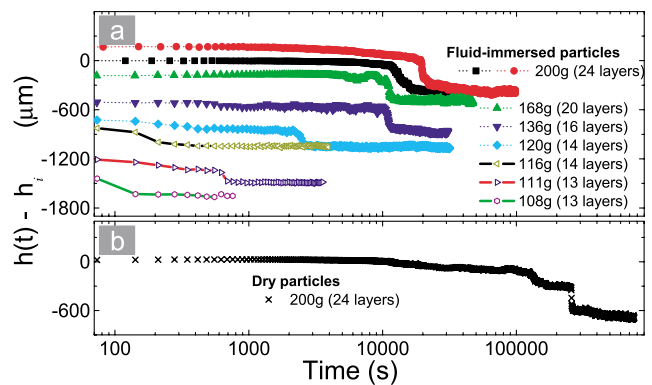


FIG. 5 (color online). (a) Compaction histories for fluid-immersed grains of different layer thickness, as indicated by the total mass of granular material (and the number of layers in the final state). The curves are shifted vertically for clarity. The transition delay grows rapidly with depth. (b) Compaction history of dry grains. In all cases, the boundary speed is 12 d/s .

demonstrates the typical compaction histories, all driven at $12 d/s$, but with different amounts of glass beads in the system. Note the logarithmic time axis. The time and boundary displacement required to produce the compaction event grows dramatically with the layer thickness. This increased time may be a result of the dramatically slower motion in the deeper layers: particles must be displaced with respect to neighbors by about one diameter in order to crystallize. This condition is equivalent to an accumulated strain comparable to unity, which occurs at the bottom for a filling of 24 layers when the integrated displacement at the top is about $10^5 d$. Thus, the internal ordering of this system, with its strongly nonlinear velocity profile and nonlinear strain accumulation, can be substantially different from thermal systems such as colloidal suspensions, where the flow profile is usually linear. For fillings of less than 13 layers, the time or boundary displacement for reaching the final volume is rather short and can be undetectable.

We have also performed the experiment in the absence of interstitial fluid and monitored the compaction, shown as Fig. 5(b). We find that the delayed step transition is generic with or without fluid. However, for the same thickness and driving speed, the characteristic transition delay of a dry granular packing can be longer by an order of magnitude (days, or $10^6 d$ in terms of boundary displacement); the transition in the dry case can occur by means of multiple compaction steps, possibly involving material at different depths. This observation suggests that friction plays a significant role in the underlying dynamics. Beyond friction, the effect of the fluid should be negligible, since the fluid drag forces are always small compared to gravitational and shear contact forces.

We can also shear the grains at a constant volume instead of constant load. In constant-volume shearing, grains still crystallize, as long as one lowers the upper plate when sufficient compaction has occurred to create a gap between grains and the shearing surface. Therefore, a large imposed load is not essential for ordering.

To summarize, we have investigated both the internal spatial structure and the time evolution of a deep granular flow in a circular channel. A steep compaction step and simultaneous rise in the amplitude of a spectral peak identify a well-defined crystallization transition. The disordered and ordered states have distinct flow rheology: the ordered state consists of sliding hexagonal planes with nearly uniform motion parallel to the shearing velocity despite the strong vertical decay in its magnitude, while the disordered flow is nearly Poiseuille-like (with some boundary slip). The ordering occurs with and without interstitial fluid, and is destroyed by sufficient polydispersity.

However, understanding the role of polydispersity will require further work, because shear-induced segregation also occurs. In a subsequent paper, we also show that the crystallization can be prevented by using a rougher lower boundary, but can then be restored by reversing the shear direction a few times initially.

This work demonstrates that slowly sheared granular flows can show complex time-dependent rheology, and that surprisingly long times may be needed to reach a steady state for deep layers. An interesting direction for future research is clarification of what internal changes control (or occur during) the slow precursor to the compaction step. Movies of internal grain motions are available on the internet [15].

The authors appreciate fruitful discussions with T. Lubensky, J. Brady, I. Aranson, L. Tsimring, and experimental assistance by K.-H. Lin *et al.* (Penn). This work is supported by the NSF Division of Materials Research under Grants No. DMR-0072203 to Haverford College, and No. DMR-0079909 to University of Pennsylvania (J. C. T.).

-
- [1] D. Muth *et al.*, *Nature* (London) **406**, 385 (2000).
 - [2] T. Komatsu, S. Inagaki, N. Nakagawa, and S. Nasuno, *Phys. Rev. Lett.* **86**, 1757 (2001).
 - [3] L. Silbert, G. Grest, S. Plimpton, and D. Levine, *Phys. Fluids* **14**, 2637 (2002).
 - [4] L. Silbert *et al.*, *Phys. Rev. E* **64**, 051302 (2001).
 - [5] G. Debregeas and C. Josserand, *Europhys. Lett.* **52**, 137 (2000).
 - [6] I. Aranson and L. Tsimring, *Phys. Rev. E* **65**, 061303 (2002).
 - [7] M. Srinivasa, K. Rao, and P. Nott, *J. Fluid Mech.* **457**, 377 (2002).
 - [8] J. Erpenbeck, *Phys. Rev. Lett.* **52**, 1333 (1984).
 - [9] J. Lutsko, *Phys. Rev. Lett.* **77**, 2225 (1996).
 - [10] W. Polashenski, P. Zamankhan, S. Makiharju, and P. Zamankhan, *Phys. Rev. E* **66**, 021303 (2002).
 - [11] A. Sierou and J. Brady, *J. Rheol.* **46**, 1031 (2002).
 - [12] S. Paulin, B. Ackerson, and M. Wolfe, *Phys. Rev. E* **55**, 5812 (1997).
 - [13] M. Haw *et al.*, *Phys. Rev. E* **58**, 4673 (1998).
 - [14] O. Pouliquen, M. Nicolas, and P. D. Weidman, *Phys. Rev. Lett.* **79**, 3640 (1997).
 - [15] See http://www.haverford.edu/physics-astro/gollub/internal_imaging/ for movies of internal grain motions. For archival purposes, they are also available as EPAPS Document No. E-PRLTAO-91-067331, which can be retrieved from the EPAPS homepage (<http://www.aip.org/pubservs/epaps.html>).